HHS Public Access

Author manuscript

Bioconjug Chem. Author manuscript; available in PMC 2019 November 21.

Published in final edited form as:

Bioconjug Chem. 2018 November 21; 29(11): 3626–3637. doi:10.1021/acs.bioconjchem.8b00564.

Vascular Targeting of Radiolabeled Liposomes with Bio-Orthogonally Conjugated Ligands: Single Chain Fragments Provide Higher Specificity than Antibodies

Elizabeth D. Hood[*,†], **Colin F. Greineder**[†], **Tea Shuvaeva**[†], **Landis Walsh**[†], **Carlos H. Villa**[†], **Vladimir R. Muzykantov**[†]

[†]Department of Systems Pharmacology and Translational Therapeutics, Perelman School of Medicine, 3400 Civic Center Boulevard, Bldg 421, Philadelphia, Pennsylvania 19104-5158, United States

Abstract

Liposomes are a proven, versatile, and clinically viable technology platform for vascular delivery of drugs and imaging probes. Although targeted liposomes have the potential to advance these applications, complex formulations and the need for optimal affinity ligands and conjugation strategies challenge their translation. Herein, we employed copper-free click chemistry functionalized liposomes to target platelet-endothelial cell adhesion molecule (PECAM-1) and intracellular adhesion molecule (ICAM-1) by conjugating clickable monoclonal antibodies (Ab) or their single chain variable fragments (scFv). For direct, quantitative tracing, liposomes were surface chelated with ^{111}In to a >90% radiochemical yield and purity. Particle size and distribution, stability, ligand surface density, and specific binding to target cells were characterized *in vivo*. Biodistribution of liposomes after IV injection was characterized in mice using isotope detection in organs and by noninvasive imaging (single-photon emission computed tomography/computed tomography, SPECT/CT). As much as 20–25% of injected dose of liposomes carrying PECAM and ICAM ligands, but not control IgG accumulated in the pulmonary vasculature. The immunospecificity of pulmonary targeting of scFv/liposomes to PECAM-1 and ICAM-1, respectively, was 10-fold and 2.5-fold higher than of Ab/liposomes. Therefore, the combination of optimal ligands, benign conjugation, and labeling yields liposomal formulations that may be used for highly effective and specific vascular targeting.

Graphical Abstract

[*]**Corresponding Author:** ehood@pennmedicine.upenn.edu.

Author Contributions

E.D.H. and C.F.G. conceived the studies. E.D.H. and C.F.G. conducted the experiments. T.S. assisted in liposome production and characterization, G.E.C. elutions, and flow cytometry. C.H.V. conceived and advised on the radiolabeling scheme and azide radioimmunoliposome conjugation. C.F.G. and L.W. conducted the animal injections and synthesized the scFvs E.D.H., C.F.G., V.R.M. wrote/edited the manuscript.

Supporting Information

The Supporting Information is available free of charge on the ACS Publications website at DOI: 10.1021/acs.bioconj-chem.8b00564. Elution profiles (fluorescent signal versus elution volume) of click conjugation binding kinetics of fluorescent dye-DBCO to azide liposomes, elution of both free fluorescent liposomes and free IgG, and size stability study of unmodified amine and azide liposomes over 120 days (PDF)

The authors declare no competing financial interest.

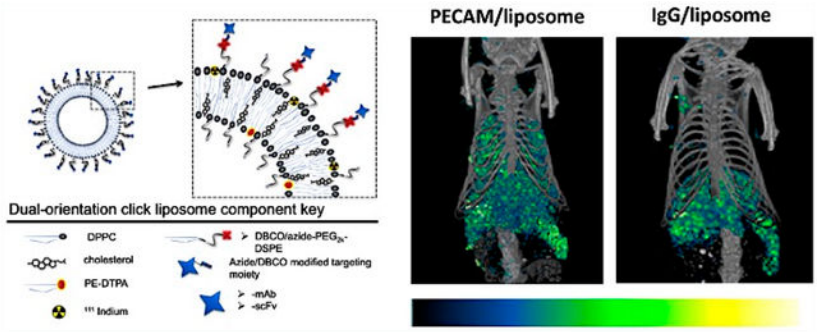

INTRODUCTION

Delivering therapeutics using affinity ligand-targeted nanoparticles has the potential to significantly alter the pharmacokinetics and therapeutic indices of small molecule drugs and biotherapeutics, enabling selective delivery of substantial payloads to areas of interest, while protecting against enzymatic breakdown, protein binding, and other sources of drug inactivation. In addition to therapeutic cargo capacity, nanocarriers provide surface area for attachment of affinity ligands, allowing high avidity binding to nearly any target accessible from the intravascular space. In the specific case of endothelial cell adhesion molecules (CAMs), like PECAM-1 (CD31) and ICAM-1 (CD54), multivalent interaction induces not only rapid binding to the vessel wall, but also clustering of surface target molecules and efficient uptake into endothelial cells (ECs).[1–6] Our laboratory and a number of others have demonstrated the potential of this approach as a means of delivering therapeutics to ECs to reverse or blunt the pathogenesis of a variety of inflammatory, ischemic, and even traumatic disease models.[1,2,7–12] For example, nanocarriers functionalized with antibody directed to the highly expressed Platelet Endothelial Cell Adhesion Molecule-1 (PECAM-1, or CD31) effectively delivered both an NADPH oxidase inhibitor[9] and an antioxidant enzyme mimetic, EUK-134,[10] to pulmonary endothelial cells *in vivo*, mitigating oxidant-induced activation and protecting the lung from endotoxin challenge. Liposomes have been the vehicle of choice for a majority of this work, given their surface area, cargo capacity, and status as the most studied and clinically successful nanocarrier.[13,14]

Despite immense potential, the benefits of this promising pharmacologic strategy have yet to be translated into clinical practice.[15] Analogous to antibody drug conjugates (ADCs), which took decades from initial conception to clinical success,[16] the seemingly straightforward notion of a targeted liposome has been challenging to put into practice. In addition to the heterogeneous physicochemical characteristics which plague all colloidal formulations, limited control over bioconjugation of affinity molecules to the liposomal surface has produced variable ligand density and orientation, aggregation, and inconsistent behavior *in vivo*. Incorporation of efficient, reproducible, and biocompatible conjugation techniques is crucial if liposomes are to achieve the same translational success as their ADC counterparts.[13,14]

Herein, we describe several steps toward this goal. We demonstrate functionalization of stable, monodisperse, and stealth liposomes for biorthogonal, copper-free click chemistry.

Both azide and cyclooctyne bearing liposomes are generated, allowing for maximum flexibility in the design and modification of targeting molecules. High efficiency conjugation is demonstrated, not only for monoclonal antibodies modified heterogeneously via traditional amine-based chemistry, but also for monomolecular and site-specific modification of recombinant single chain variable fragments (scFv). Indeed, scFv liposomes are shown to have high conjugation efficiency and remarkably consistent ligand surface density, with the end result being near-equivalent endothelial targeting relative to liposomes decorated with their parental antibodies and higher immunospecificity relative to controls. Incorporation of a radiometal chelator into these click immunoliposomes enables one-step ^{111}In labeling with >90% radiochemical yield and purity across a wide range of specific activities, allowing for both traditional “cut and count” radiotracing and noninvasive micro SPECT/CT imaging. This work sets the stage for detailed characterization of the pharmacology of these endothelial-targeted radioimmunoliposomes in both animal models and humans.

RESULTS

Dual Orientation Cu-Free Click-Functionalized Liposome Design and Characterization.

Copper-free click functionalized liposomes were formulated to accommodate ligand conjugation via strain-promoted azido-alkyne cyclo-addition of either azide or dibenzocyclooctyne (DBCO) modified targeting species. First, in the DBCO functionalized formulations (Figure 1a) we included 6% amine PEG_{2000} DSPE (1,2-distearoyl-*sn*-glycero-3-phosphoethanolamine) in a mole ratio 25% cholesterol to 75% phospholipid (DPPC less 0.2% DTPA for ^{111}In inclusion, or 0.5 mol % Top FL-PC for FL tracing) at 20 mM total lipid concentration using traditional thin film extrusion methods.[9] The amine-functionalized liposomes were then reacted with 120 μM NHS PEG_4 DBCO. (We found that direct DBCO functionalization of liposomes through the inclusion of DBCO-PEG DSPE lipid at any concentration or viable ratio of our formulations of cholesterol:phospholipid or additions of mPEG-DSPE resulted in large, polydisperse liposomes that rapidly aggregate.) The extent of the DBCO NHS labeling to the amine PEG DSPE in formed liposomes was first tested using fluorescein azide (SI Figure 1). Once the primary DBCO functionalization of the amine PEG liposome was verified, they were reacted with azide modified IgG. The hydrodynamic radius and effect of each modification on the particle size and distribution index (PDI) was monitored at each step. Figure 1b shows a representative particle size distribution based on population number versus diameter size from dynamic light scattering (DLS) measured in 100-fold diluted samples which maintains a consistent size distribution and PDI at each step of modification. Observations from numerous experiments consistently result in a slight increase in size at each step, from ~130 ± 15 nm after filter extrusion to 150 ± 20 nm after the DBCO PEG_4 NHS ester reaction, and finally to ~180 ± 20 nm with the addition of IgG-azide). Similarly the PDI increased from less than 0.1 to less than 0.2 to close to 0.3 at each corresponding step.

Azide functionalized liposomes were synthesized directly using the same formulation but substituting an azide PEG_{2000} DSPE for the amine linker (Figure 1c). Observations from numerous experiments repeatedly showed an increase from ~135 ± 10 nm after filter

extrusion to 150 ± 20 nm after the addition of IgG-DBCO as evident in the particle size distribution curves in Figure 1d. Similarly the PDI increased from less than 0.1 to less than 0.2 correspondingly. The azide liposome + DBCO ligand pairing consistently resulted in a smaller-sized particle and a narrower PDI; however, the use of a more soluble strained cyclooctyne in the amine + DBCO formulation might resolve this difference.[17]

The capacity of the DBCO functionalized liposomes to conjugate targeting ligands was verified and quantified by tracing a radiolabeled IgG-azide or scFv-azide via gel exclusion chromatography, separating particle bound ligands from unbound. In Figure 2a, the elution data indicate that ~90% of the labeled scFv or mAb-azide signal is found in the fractions captured in the first peak (5.5–7 mL), consistent with where liposomes elute (SI Figure 2). The number of ligands bound shown in the ordinate axis in Figure 2a was calculated as proportional to the area under the curve of the elution traces relative to the known quantity of radiolabeled ligands added. Analogous experiments with azide functionalized liposomes conjugating 125I-radiolabeled IgG-DBCO or scFv-DBCO shown in Figure 2b, calculated identically, yielded similar reaction efficiencies with DBCO-bearing ligands. This high reaction efficiency results in a low concentration of free ligands, which, along with increasing the yield, also reduces purification steps.

Next, we tested the reaction kinetics of our functionalized DBCO and azide liposomes with their click IgG counterparts incubating them from 15 min to overnight at 37°C and eluting them as already described (Figure 2c and d). We added approximately 200 IgG to a liposome (based on an average preconjugation liposome concentration of 2×10^{13} #/mL as previously reported[9]) and 400 scFv/liposome. In either orientation scheme, click liposomes bound 20% of added ligands within the first 15 min of the reaction. The azide liposomes showed greater binding capacity over the DBCO modified particles from 1 to 4 h, but both formulations reached near total conjugation at the longest time points (Figure 2e) showing a logarithmic relation and first-order reaction kinetics. The effects of the addition of azide/DBCO IgG on the particle size and PDI with either formulation at each time point is shown in the table in Figure 2f. The data show that both orientations demonstrate rapid and consistent conjugation of click ligands, but the azide functionalized liposomes maintain a more consistent size and a smaller PDI than the DBCO particles. These results are unsurprising since the DBCO-NHS reagent itself requires a sulfo or PEG group to be water-soluble. Attempts at adding DBCO-NHS reactive groups lacking the PEG group resulted in particles that tended to aggregate, with higher PDIs and polydispersity, as described with direct inclusion of headgroup functionalized DBCO-PEG-DSPE. Both primary particle formulations (either the pre-DBCO amine or azide functionalized) measured prior to any post extrusion modifications or purifications showed colloidal stability for up to 4 months stored in a neutral buffer at 4°C (SI Figure 3).

Hereafter, we focused our experiments on the azide functionalized liposome formulation due to more rapid throughput, greater particle stability with respect to size and PDI, and their capacity to directly accommodate radiolabeling and copper free click ligand conjugation. However, in the event that the characteristics of particular targeting ligand of choice (mAb, scFv, nanobody, or polypeptide) dictated that the addition of a strained cyclooctyne group reduced the targeting moiety’s affinity or activity, we have observed that the two-step DBCO

radioimmunoliposome is robust with respect to radiolabeling, *in vivo* affinity and specificity, and *in vivo* targeting (data not shown).

In vivo Binding.

As shown in Figure 3, we used flow cytometry to assess the binding capacity and selectivity *in vivo* to cell adhesion molecules via liposomes targeted with either parental mAb cell adhesion molecule ligands (Figure 3a,c,e), or their corresponding scFv fragment (Figure 3b,d,f) in model cell lines that stably express mouse ICAM-1, human ICAM-1, or mouse PECAM-1, respectively. In each experiment identical concentrations of CAM targeted liposomes (either mAb or scFV) were incubated with CAM cells vs wild type (WT) cells lacking target antigen.

When increasing concentrations of fluorescently labeled, targeted liposomes were added to equivalent concentrations of cell suspensions for 30 min on ice, then spun and washed, clear binding specificity is seen with little untargeted interaction of the CAM ligand liposomes in control cells. Saturation of signal can be seen in binding curves of all the mAb-CAM targeted particle experiments (Figure 3a,c,e), and with the mouse PECAM scFv liposomes (Figure 3f). Further inquiry establishing the saturation range for the mouse and human ICAM scFv liposomes in these *in vivo* model cells was outside the scope of these studies, but will be considered in future studies focused on scFv ligand to particle coating density studies with binding and localization *in vivo* and *in vivo*.

DTPA Liposome ^{111}In Labeling via High Efficiency Surface Chelation.

Liposomes designated for ^{111}In labeling included 0.2% (relative to total phospholipid) of DTPA-PE to the film solution to facilitate surface chelation.[18] Click and chelation-ready liposomes were hydrated with citrate buffer to maintain pH 4–5 optimal for chelation, which may also be more biocompatible than ammonium acetate or other applicable reported chelation media.[19] Additionally, citrate buffer is used to facilitate transmembrane pH gradient remote drug loading,[20] useful in future drug loading applications.

The overall reaction scheme is shown in Figure 4a. Briefly, the citrate-buffered ^{111}In chloride was added to DTPA azide liposomes, and after 1 h (at 37°C) incubation, free DTPA was used to quench the reaction. After buffer exchange, the radiolabeled liposomes were ready to be incubated with the targeting moiety. Radiochemical yield and purity were quantified by thin film chromatography (TLC) through both autoradiography imaging and gamma counting of the TLC silica strip. Figure 4b shows the high efficiency of radiochemical yield and consistency across feasible pH range 3–5 in both azide and pre-DBCO amine liposomes as measured by cutting and counting TLC silica gel strips, comparing the origin to the sum of the origin and the migrated fraction.

The graphs in Figure 4c,d show a quantification of the signal intensity along the strip inset above and scaled to distance with the graphs. The pH 4.5 representative data corroborate the pH 4.5 data points in Figure 4b. We calculate the theoretical maximum loading capacity of ^{111}In in our liposomes to be 93 mCi/μmol lipids based on an equimolar isotope to DTPA chelation and a specific activity of 4.19×10^5 Ci/g at DTPA 0.2 mol % total lipid. We tested a loading range of 20–500 μCi/μmol lipid, characterizing them as described above, and

found a linear relationship of chelation across the entire range (Figure 4e). The radiochemical yield and purity range from 90% to 95% as shown in Figures 4f,g. The robustness of our chelation efficiency and distance from saturation of either the addition of indium activity or the amount of membrane included DTPA chelator lipid indicate that we could accommodate much higher activity loading, useful for high activity labeling needed for cell or organ targeting and imaging applications of lower resolution epitopes.

Micro-SPECT/CT Imaging of Click Radioimmunoliposomes Targeted to PECAM.

It is well-known that the pulmonary vasculature is a preferential site of accumulation of entities with affinity to the endothelium.[1,5,21–25] To test the capacity of our formulation as a potentially viable imaging tool, we injected 100 μCi ^{111}In labeled liposome (~100 μCi/mol lipid) modified with PECAM mAb, PECAM scFv, IgG, or human scFv control intraocularly into Naïve mice, and imaged the euthanized mice 30 min post injection. SPECT/CT data from scans were 3D reconstructed and coregistered in ImageJ (version Fiji). Figure 5a shows the overlay of SPECT/CT images obtained for the PECAM mAb radiolabeled liposome, showing significant accumulation in the lungs as compared to a complete absence of signal in the lungs of the IgG/radiolabeled liposome treated mouse, seen in Figure 5b. Similarly, the corresponding PECAM scFv liposomes demonstrate a clear lung signal compared to the control scFv in Figure 5d. These data largely corroborate the biodistribution data that follows, and demonstrate the utility of the click ligand targeted radiolabeled liposome as an imaging tool.

PECAM- and ICAM-Directed Targeting to the Pulmonary Vasculature: scFv/Liposomes Specificity Surpasses mAb/Liposomes.

Finally, we appraised the targeting features of the CAM-targeted liposomes *in vivo*. Previous studies established that antibodies and antibody-coated nanoparticles targeted to PECAM-1 and ICAM-1 accumulate in the lungs of animals rapidly (i.e., within 10–30 min) after intravenous injection.[8–11,26,27] This phenomenon reflects both the large vascular surface in the lungs exposing these antigens directly to circulating blood and the exclusive perfusion of the lungs, as the only organ receiving more than 50% of total systolic blood volume ejected from the ventricles.[7] Therefore, the pulmonary accumulation of mAb/liposomes normalized to control IgG/liposomes may be used to quantitatively characterize specific targeting.

In the data in Figure 6 we quantified the biodistribution of ^{111}In-labeled immunoliposomes 30 min after injection in mice. Figure 6a shows that liposomes targeted to PECAM-1 by either mAb or scFv specifically accumulate in the lungs, 120% and 100% ID/g, respectively (corresponding to ~25% and 20% ID/organ). In control animals, pulmonary uptake of nontargeted IgG/liposomes and scFv/liposomes did not exceed 10% ID/g and 3% ID/g, respectively. Interestingly, the markedly lower (3-fold) level of the pulmonary uptake of nontargeted scFv/liposomes vs IgG/liposomes was not due to a lower blood level. In fact, the blood level of untargeted scFv/liposomes was markedly higher (3-fold) than mAb/liposome counterpart. Therefore, the lung/blood ratio (Localization Ratio, or LR) of untargeted control scFv/liposomes was about 10-fold lower than IgG/liposomes.

This resulted in marked changes of the immunospecificity index (ISI, the ratio of the targeted to control counterpart normalized to blood level, i.e., the ratio of targeted to untargeted LR). In fact, the ISI of the pulmonary targeting of anti-PECAM scFv/liposomes and mAb/liposomes (Figure 6b) was 8-fold higher for the former formulation. This effect was observed in the lungs, but not in other organs. For example, the uptake in liver was higher for whole immunoglobulin carrying liposomes, likely due, at least in part, to the presence of Fc-fragments in the liposome-coupled IgG and mAb. This pattern was reproduced nearly identically in the animals injected with ICAM-targeted mAb/liposomes and scFv/liposomes, indicating that this may be a generalizable phenomenon (Figure 6c,d).

DISCUSSION

The development of a clinically viable targeted nanocarrier necessitates consistent and reproducible refinements of ligand conjugation efficiency and orientation uniformity, biocompatibility, and a universality of bioconjugation schemes across all ligand types (e.g., monoclonal Abs, mAb; single chain variable fragments, scFv, and other affinity ligand derivatives). Such a goal necessitates that the bioconjugation scheme be rapid, efficient, and minimizing of the product's heterogeneity and purification steps. Previous work from our lab, and others, has demonstrated that drug carriers with affinity for vascular endothelial cells are well suited to reverse disease pathogenesis and boost endogenous vasculo-protective mechanisms.[2,6,8–10] Liposomal nanocarriers are of particular interest as the most developed and, thus far, clinically applicable nanoparticle.[13,14] In prior work, we reported that mAb functionalized immunoliposomes targeted to the constitutively expressed endothelial cell adhesion molecule, PECAM-1, effectively delivered both an NADPH oxidase inhibitor[9] and an antioxidant enzyme mimetic, EUK-134,[10] protecting the lung from cytokine induced inflammation and injury. Capitalizing on our prior results, we sought to adapt our nanocarrier formulation to support scFv targeting as well as mAb, and to enable a direct and equivalent comparison of the individual ligands immunoliposome targeting efficacy.

Monoclonal antibodies (mAbs) have been used extensively as the key targeting moiety in much of vascular targeting research[3,22] since they tolerate chemical modifications with little effect on affinity, and demonstrate prolonged vascular circulation.[28] Disadvantages, however, include their size, potential for Fc fragment mediated immunogenicity, or antigen cross-linking that may impede the clinical translation of mAb as nanoparticle targeting ligand. As an alternative, antibody-derived single-chain variable fragments (scFv) have been shown to retain affinity characteristics of parental mAb but lack the constant domains of antibody heavy and light chains responsible for some mechanisms of clearance and immune system activation.[29] Additionally, the recombinant construction of scFv results in site-specifically oriented, homogeneous products that enable directed and consistent ligand orientation. We have demonstrated the scFv utility and targeting capacity via a peptide-mediated click conjugation to the antioxidant enzyme catalase.[30] As reported, we observed that smaller, recombinant, endothelial-specific affinity ligands, including scFv, are vulnerable to affinity changes when using amineand thiol-based conjugation chemistries, motivating us to adapt our immunoliposome conjugation strategy to click chemistry.

Although previously described biotin/streptavidin (SA) and maleimide/SATA (succinimidyl *S*-acetylthioacetate) conjugation approaches provide ample conjugation and targeting, both approaches have translational limitations. Biotin/SA binding is noncovalent, and the inclusion of streptavidin creates immunogenicity issues.[31] Overcoming the SA multivalency[32] requires inherent stoichiometric inefficiencies when added to biotinylated nanocarriers to avoid possible cross-linking.[33] The widely used thiol/maleimide bioconjugation schemes include reactants that are vulnerable to oxidation and require lengthy deprotection steps, exposing the reactive thiol group prior to conjugation of maleimide functionalized particle to thiol-ligand. Additionally, the nonspecific thiol/maleimide functionalization of ligands for particle conjugation is limited to fulllength mAbs; the affinity of scFv and mAb derivatives are challenged under these conditions, depending on the amino acid sequence and the accessibility of modifiable lysine residues.[30]

Recent interest in click chemistry techniques applied to nanoparticle and targeted therapeutics has increased substantially due to several desirable attributes, including biological specificity and chemical selectivity.[34–36] Initial applications of click conjugation in liposomes used copper catalyzed azide–alkyne cycloaddition as described by Schuber.[37] In an alternative to copper catalyzed reactions, liposomes were surface modified using the Staudinger ligation method, in which a phosphine group is reacted with an azide to form an amine covalent bond.[38] Both approaches had drawbacks; the residual copper catalyst is toxic to cells and interferes with protein activity,[39] and the phosphine reaction kinetics are slow, and vulnerable to oxidation.[17] However, more recent click chemistry ligand functionalization techniques have migrated toward copper-free strain-promoted azido-alkyne cycloaddition reactions, avoiding the potentially cytotoxic effects of the copper catalyst,[40] and improving reaction kinetics.[17,41] None of the previous approaches demonstrated the yield purity or the specificity of covalent bioorthoganal conjugation, while allowing control of ligand orientation, especially with respect to site-specifically engineered targeting ligands.[30,42] This novel azide liposome formulation creates a nanocarrier that is stable, monodisperse, readily radiolabeled and ligand conjugated, providing a consistent elution profile at each stage of modification. The bioconjugation kinetics of targeting ligands were rapid, first order, and highly consistent, allowing for a controllable titration of ligand density on the particle. *In vivo* verification of click immunoliposome specific binding to adhesion molecule presenting cells demonstrated high specificity and robust, rapid binding in human and mouse cell lines using scFv and mAb targeting of PECAM and ICAM.

Radiotracing of nanoparticles *in vivo* is a powerful translational medicine and clinical research tool. By SPECT/CT or PET technologies, molecular imaging allows the noninvasive quantification of localized carriers and cargo to sites of interest. Our prior research showed specific imaging to a pathological vascular bed in an inflamed mouse model, targeting ICAM with polymeric nanoparticle (NP) probes.[27] A key element in the success of this PET imaging platform was the capacity of the NP to be directly radiolabeled, rather than the effective, but more limiting practice of doping in a nonspecific, radiolabeled ligand on the nanoparticle surface for tracing. Tracing a fraction of the ligand population rather than the particle itself necessitates limiting the amount of tracer to avoid crowding out the targeting ligand, which also potentially hampers the affinity of the targeting overall, especially in the case of antibody derivatives such as scFv.[29,30] Adapting immunoliposomes

to be radiolabeled highly efficiently and robustly via inclusion of a surface chelator[18] within a liposome bilayer capitalizes on our previous insights, while creating biocompatible, drug cargo vehicles with real potential for clinical utility.

The vascular selectivity was further demonstrated *in vivo* using both imaging and biodistribution of ^{111}In labeled CAM targeted click liposomes. Endothelial specificity of adhesion molecule targeting to both PECAM-1 and ICAM-1 is evidenced by the pulmonary uptake seen in the SPECT/CT and the biodistribution data. Notably, the rapid blood clearance of the radioimmunoliposomes seen in the biodistribution and imaging data demonstrates a high signal-to-noise (S/N) ratio relative to nonendothelial targets reported elsewhere.[18] This facility, coupled with the capacity of the formulation to chelate orders of magnitude higher activity, would potentially permit identification of less abundant endothelial epitopes that may be highly localized.[43,44]

Most notably is the click bioconjugation method's benign impact on the innate affinity of the targeting ligands, especially that of scFv, long understood to be vulnerable to compromise by chemical modification. That is in contrast to the more robust nature of the mAb, and only by using an unimpaired scFv can the elucidation of the effects that the Fc effector domain may have on parental mAb-IL targeting and pharmacokinetics vs that of the scFv be revealed, as demonstrated by ISI data. To this point, although the pulmonary distribution was similar for both PECAM and the ICAM mAb and scFv radioimmunoliposome targeting, analysis of the ISI ratio of control to immunotargeted particles revealed greater specificity in both scFv cases.

This remarkable and novel finding has several possible explanations, as listed below without order of priority. First, the molar addition of scFv conjugated to liposomes is twice that of mAb, yielding liposomes carrying more molecules scFv than Ab. However, since each mAb has two binding sites, then the steric limitations imposed by conjugation to the liposome on engagement to the target by the large and flexible mAb molecule might be expected to be less than those of scFv. On the other hand, the avidity of the scFv/liposome versus the mAb/liposomes *in vivo* and *in vivo* can be higher due to reduced inactivation by the site-specific modification of the scFv[29] directing optimal orientation with respect to ligand alignment on the surface of the nanoparticle.[30]

CONCLUSION

These data describe a nanoparticle formulation that is easily radiolabeled, and rapidly and efficiently conjugates both mAb and scFv targeting ligands, while maintaining a consistent size and PDI. The click radioimmunoliposomes bind rapidly and specifically to targets, *in vivo* and *in vivo*, and demonstrate a robust utility for molecular imaging. The microSPECT/CT imaging data shown demonstrate proof-of-principle as a molecular imaging tool, and confirm the capacity of the click radioimmunoliposome to clearly identify a targeted molecular marker in an uninjured vascular bed within 30 min with low systemic background. These click radioimmunoliposomes facilitate the direct comparison of scFv and parental mAb nanoparticle targeting without adverse effects to the affinity of the scFv by nonspecific chemical modifications. The potential utility of a clinically viable drug delivery

vehicle that can be functionalized to accommodate covalent, bioorthogonal conjugations of adaptable targeting ligands and be non-invasively traced *in vivo* is far-reaching. Our ongoing research directions with this promising and versatile nanoparticle formulation includes characterizing and optimizing drug cargo loading and therapeutic efficacy in acute models of injury, specifying affinity to defined molecular targets *in vivo* and *in vivo* relative to ligand coating density and mAb orientation, and defining potentials for toxicity or immunogenicity with respect to the characterized variables.

EXPERIMENTAL PROCEDURES

Ethics Statement.

Animal studies were carried out in accordance with the Guide for the Care and Use of Laboratory Animals as adopted by the NIH, under protocol nos. 805696 and 805708 approved by University of Pennsylvania IACUC.

Cell Lines.

Multiple cell lines were used for production of mAb and scFv targeting ligands, and for *in vivo* binding and affinity assays testing CAM targeted click radioimmunoliposomes. Mouse and human anti-ICAM-1 and anti-PECAM mAbs were produced by culturing hybridomas (clones YN1/1.7.4, R6.5, and 390, respectively)[8,45,46] and purified using protein G sepharose fast flow (GE Healthcare Life Sciences, Pittsburgh, PA). The stable cell lines, REN-mICAM and REN-mPECAM, and the wild type REN mesothelioma cell line, were maintained as previously described.[8] Chinese hamster ovary cells (CHO) stably transfected with recombinant human ICAM-1 and wild type control CHO cells were purchased from ATCC (Manassas, VA). To generate cells for flow cytometry and immunoreactivity assays, confluent cells were trypsinized (0.05% trypsin, 0.02% EDTA; Sigma-Aldrich, St Louis, MO), fixed in a 2% solution of paraformaldehyde for 5 min on ice, washed with sterile 1× PBS, resuspended in 10% DMSO/2% FBS, and stored in aliquots at −80°C.

NHS Ester-Mediated Azide/DBCO Modification of Targeting Immunoproteins.

IgG and mAb were modified with dibenzylcyclooctyne-PEG_4-NHS ester (Jena Bioscience; Thuringia, Germany). The proteins, buffered in PBS and adjusted to pH 8.3 with 1 M $NaHCO_3$ buffer, were reacted for 1 h at room temperature (RT) at a ratio of 1:10 mAb/NHS ester PEG_4 DBCO. Post reaction, the mixture was buffer exchanged with an amicon 10k MWCO centrifugal filter (MilliporeSigma, Burlington MA) to remove unreacted NHS ester PEG_4 DBCO. The extent of modification was quantified by labeling the purified IgG-PEG4-DBCO product with fluorescent azide dye (FAM-azide 5 isomer; AbCam, Cambridge, MA) at 1:10 molar ratio for 1 h at RT. Unreacted FAM-azide was removed with an extensively rinsed (to remove sodium azide storage solution) desalting column (zeba spin desalting column; Thermo Scientific, US) and the fluorescent azide concentration was quantified by comparison to a linear calibration curve of free dye, measured on a fluorescent plate reader (Spectramax M2; Molecular Devices, San Jose, CA). Calculating the ratio of the fluorescence concentration relative to the protein concentration (measured by absorbance at 280 nm using a Nanodrop Microvolume Spectrophotometer, (ThermoFisher, US)) indicated the extent of modification of the protein, usually between 1 and 3 groups/molecule. Azide

modification of IgG/mAb was carried out similarly, instead using NHS ester-PEG_4-azide and Alexafluor 488-DIBO alkyne (both from Thermo Scientific, US).

For tracing ligand to liposome conjugation, IgG-DBCO or IgG-azide underwent radio-iodination with Na−^{125}I using the iodogen method as already described.[30]

Production of Sortagged Recombinant Affinity Ligands.

Molecular engineering and site-specific modification of endothelial CAM-targeted single chain antibody fragments (scFv) have been described previously.[29,30,45] In previous reports, these proteins were produced in drosophila S2 cells. Here, cDNAs encoding the same C-terminal sortagged and triple-FLAG tagged scFv proteins were cloned into the pBAD/gIII B vector (ThermoFisher Scientific) between *NcoI* and *XbaI* restriction enzyme sites for periplasmic expression in *E. coli*. Bacteria were grown to appropriate density and induced overnight with 0.02% arabinose at 18°C. Recombinant proteins were released from the periplasmic space by osmotic shock and purified via affinity chromatography using a L5 agarose column (BioLegend, San Diego CA).

Preparation of DBCO-Modified GG Peptide and Site-Specific Modification of scFv.

To allow oriented conjugation of sortagged affinity ligands to azide liposomes, we first prepared a fluorescently labeled peptide with C-terminal DBCO. A peptide with sequence NH_2-GGGK(FAM)GGSC-CO_2 was purchased from Pierce Custom Peptides (Thermo-Fisher Scientific), resuspended in degassed 0.1 M phosphate buffer pH 7.0, and reacted for 2 h at RT with sulfo DBCO-PEG_4-maleimide (Click Chemistry Tools, Scottsdale, AZ) in a final concentration of 10% DMSO. The reaction product was separated from the components using a Sep Pak C18 Cartridge (Waters, Milford, MA) and purity was verified by demonstrating a single peak on reverse phase HPLC. A 5-fold excess (50 μM) of the DBCO-modified peptide was then conjugated to sortagged scFv (10 μM) by reacting the latter with an equimolar concentration of sortase in the presence of 1 mM $CaCl_2$ at RT overnight, as previously described.[8] 6xHis-tagged sortase was removed by incubation with Ni-NTA agarose (Qiagen, Germantown, MD). Excess peptide was removed by 10 kDa MWCO Amicon centrifugal filter. Purity of modified protein was confirmed by SDS-PAGE and/or size exclusion HPLC.[8]

Synthesis and Characterization of Dual Oriented Click Immunoliposomes.

Radioimmunoliposome Synthesis and Characterization.—Azide and amine functionalized liposomes were prepared by thin film hydration techniques similar to those previously described.[9] Briefly, lipids DPPC (1,2-dipalmitoyl-*sn*-glycero-3-phosphocholine), cholesterol, and either amine PEG_{2000} DSPE (1,2-distearoyl-*sn*-glycero-3-phosphoethanolamine) or azide PEG_{2000} DSPE (1,2-distearoyl-*sn*-glycero-3-phosphoethanolamine-*N*-[azido(polyethylene glycol)-2000]) (All phospholipids purchased from Avanti Polar Lipids, Alabaster, AL) in chloroform were combined in a borosilicate glass tube at a total lipid concentration of 20 mM with the phospholipid to cholesterol ratio at 3:1, using 6% of phospholipid mass for linker. Additionally, liposomes fated for^{111} In radiolabeling include 0.2 mol % DTPA-PE (1,2-distearoyl-*sn*-glycero-3-phosphoethanolamine-*N*-diethylene-triaminepentaacetic acid), and those requiring

fluorescence include 0.5 mol % Top FL-PC (1-palmitoyl-2-(dipyrromethene boron difluoride)undecanoyl-*sn*-glycero-3-phosphocholine). This translates to a standard composition of 68.8% DPPC, 25% cholesterol, 6% azide-PEG2k-DSPE, and 0.2% DTPA-PE for the radioimmunoliposome formulation. Lipid solutions were subjected to a constant stream of nitrogen gas until visibly dried then lyophilized for 1–2 h to remove any residual solvent. Dried lipid films were hydrated with buffer (sterile Dulbecco's phosphate buffered saline (hereafter PBS), or 0.3N metal free citrate pH 4), then went through 3 freeze–thaw cycles using liquid N_2/50°C water bath then extruded 10 cycles through 200 nm polycarbonate filters (Avanti Polar Lipid). Dynamic light scattering measurements of hydrodynamic particle size, distribution, and PDI were taken at each step of formulation from extrusion and subsequent modifications at 1:125 dilution in PBS using a Zetasizer Nano ZSP (Malvern Panalytical, Malvern UK).

Ligand Conjugation and Characterization of Click Immunoliposomes.

For DBCO reactive liposomes, the click functionalization preparation took place in two steps, as shown in Figure 1a. The amine bearing liposomes were reacted with DBCO PEG NHS ester in DMSO at 15 mM (Jena Scientific) to final concentration of 120–180 μM for 2 h at RT with rotation, then purified by washing with a 10k MWCO Amicon centrifugal filter for 20× volume exchanges. Verification of DBCO modification was tested by reacting a small aliquot of the functionalized liposomes with FAM-azide, as described above for IgG-DBCO modification, adding 1 mM FAM azide to a 6–10× molar excess, then quantifying extent of reaction with size exclusion chromatography using Sepharose 4B−Cl (GE Healthcare, Pittsburgh PA) packed in a 20 mL Biorad polyprep column taking 0.5 mL fractions for 25 mL, and plating a portion of each fraction on a 96 well plate to be read on a plate reader at λex/em = 493/525. Once the DBCO surface modification was verified, azide functionalized IgG (or mAb/scFv) were incubated with DBCO modified IL at 37°C for designated times (time studies 15 min to overnight). After incubation, the reaction mixtures were characterized and purified using size exclusion chromatography (as previously described) with quantification via tracing ligand fluorescence or radioactivity (read each fraction on a gamma counter). Efficiency of conjugation reaction is quantitatively defined as the ratio of the area under the curve of the ligand signal in the liposome peak (4.5−6 mL) over the integration of the entire 25 mL elution.

Surface Chelation Radiolabeling of Liposomes.

All radiolabeling chelation reactions were performed using metal free conditions to prevent contaminating metals from interfering with DTPA. Metals were removed from buffers using Chelex 100 metal affinity resin (Biorad, Laboratories, Hercules CA). Varying amounts (20−500 μCi/μmol phospholipid) of $^{111}In{-}Cl_3$ (Nuclear Diagnostic Products, Cherry Hill, NJ) diluted in citrate buffer were added to preformed azide 0.2% DTPA liposomes that had been hydrated with metal-free pH 4 citrate buffer for 1 h at 37°C as previously described.[18] The reaction mixture was quenched with 50 mM DTPA to 1 mM final concentration to chelate unincorporated ^{111}In. The radiochemical purity and yield was measured using thin film chromatography (TLC) with mobile phase EDTA 10 μM and quantified via phosphor imaging and gamma counting of the aluminum silica strips (Sigma Chemical, St Louis MO).

For *in vivo* SPECT/micro CT imaging experiments liposomes were labeled with 100 μCi/μmol lipid, and for biodistributions were labeled at 50 μCi/μmol. Samples were buffer exchanged with sterile 1× DPBS using Amicon centrifugal filters, followed by targeting ligand conjugation as described above, prior to injections.

Click Immunoliposome Cell Binding by Flow Cytometry.

REN and CHO cells, either fixed (REN mouse ICAM/WT, CHO human ICAM/K) or live (REN mouse PECAM/WT), were grown as described. Cell aliquots of ~100k were prepared in duplicates. Serial dilutions of click fluorescent immunoliposomes bearing either scFv or mAb against ICAM or PECAM were incubated with both adhesion molecule bearing cells and control cells for 30 min on ice. Samples were centrifuged and washed 2× with complete media and resuspended in 100 μL. Flow cytometry (Accuri C6; BD Biosciences, Franklin Lakes, NJ) measurements were made sorted on free cells populations and FL1. Averaged median data of FL1 in each sample were graphed.

Micro-SPECT/CT Imaging.

Thirty minutes after injection of ~100 μCi click radioimmunoliposomes, the mouse was placed into the MiLabs U-SPECT (Utrecht, Netherlands) scanner bed. A region covering the entire body of the animal was selected and scanned using the listmode acquisition of the scanner for 90 min. At the completion of the scan, the animal was moved to the MiLabs U-CT (Utrecht, Netherlands) for a CT scan covering the entire body of the animal using the default acquisition (240 μA, 50 kVp, 75 ms exposure, 0.75° step with 480 projections). The SPECT data was reconstructed using the reconstruction program provided by the manufacturer using 400 μm voxels. The CT data were reconstructed using the reconstruction provided by the manufacturer using 100 μm voxels. Data processing was done using ImageJ software (FIJI version 2.2.2-rc-67/1.52c) holding each sample SPECT data set to a standard threshold value range and region of interest (ROI). Using a 3D plugin model program within the FIJI software, the SPECT and CT data were overlaid, and pseudocolor was applied to give scale to the SPECT signal.

Biodistribution of Click Radioimmunoliposome.

Naïve C57BL/6 male mice (The Jackson Laboratory, Bar Harbor, ME) anesthetized with ketamine/xylazine (100/10 mg/kg) were injected intraocularly with 1 μmol (0.75 mg) total lipid click radioimmunoliposome conjugated with targeting ligand against ICAM or PECAM mAb or scFv and corresponding control (IgG or human scFv respectively). Animals were euthanized 30 min after injections; the organs of interest harvested, rinsed with saline, blotted dry, and weighed. Radioactivity in organs and ~100 μL blood was measured with a Wallac 1470 Wizard gamma counter (PerkinElmer Life and Analytical Sciences-Wallac Oy, Turku, Finland). The gamma data of the ^{111}In measurements and organ weights were used to calculate the tissue biodistribution injected dose per gram. The total injected dose was measured prior to injections, corrected for tube and syringe residuals, and verified to be ≥80% of the sum of the individual measures.

Supplementary Material

Refer to Web version on PubMed Central for supplementary material.

ACKNOWLEDGMENTS

Many thanks to Eric Blankenmyer at the small animal imaging facility at Perelman School of Medicine, University of Pennsylvania for MicroSPECT/CT measurements and raw data and Dr Raisa Kiseleva for cell lines. This work was supported by the National Institute of Health grant nos. R01-HL-128398 (E.D.H, V.R.M.), R01-HL-126874 (V.R.M.), and T32 HL007439 (C.F.G.).

ABBREVIATIONS

CT	computed tomography
DBCO	dibenzylcyclooctyne
ECs	endothelial cells
ICAM	intercellular adhesion molecule
PECAM	platelet– endothelial cell adhesion molecule
PEG	polyethylene glycol
scFv	single-chain antibody fragments
SPECT	single-photon emission computed tomography

REFERENCES

(1). Chacko AM, Hood ED, Zern BJ, and Muzykantov VR (2011) Targeted Nanocarriers for Imaging and Therapy of Vascular Inflammation. Curr. Opin. Colloid Interface Sci 16 (3), 215–227. [PubMed: 21709761]

(2). Greineder CF, Brenza JB, Carnemolla R, Zaitsev S, Hood ED, Pan DC, Ding BS, Esmon CT, Chacko AM, and Muzykantov VR (2015) Dual targeting of therapeutics to endothelial cells: collaborative enhancement of delivery and effect. FASEB J 29 (8), 3483–3492. [PubMed: 25953848]

(3). Howard M, Zern BJ, Anselmo AC, Shuvaev VV, Mitragotri S, and Muzykantov V (2014) Vascular targeting of nanocarriers: perplexing aspects of the seemingly straightforward paradigm. ACS Nano 8 (5), 4100–32. [PubMed: 24787360]

(4). Kiseleva RY, Glassman PM, Greineder CF, Hood ED, Shuvaev VV, and Muzykantov VR (2018) Targeting therapeutics to endothelium: are we there yet? Drug Delivery Transl. Res 8 (4), 883–902.

(5). Muzykantov VR (2005) Biomedical aspects of targeted delivery of drugs to pulmonary endothelium. Expert Opin. Drug Delivery 2 (5), 909–26.

(6). Shuvaev VV, Brenner JS, and Muzykantov VR (2015) Targeted endothelial nanomedicine for common acute pathological conditions. J. Controlled Release 219, 576–595.

(7). Brenner JS, Greineder C, Shuvaev V, and Muzykantov V (2015) Endothelial nanomedicine for the treatment of pulmonary disease. Expert Opin. Drug Delivery 12 (2), 239–61.

(8). Greineder CF, Chacko AM, Zaytsev S, Zern BJ, Carnemolla R, Hood ED, Han J, Ding BS, Esmon CT, and Muzykantov VR (2013) Vascular immunotargeting to endothelial determinant ICAM-1 enables optimal partnering of recombinant scFv-thrombomodulin fusion with endogenous cofactor. PLoS One 8 (11), e80110. [PubMed: 24244621]

(9). Hood ED, Greineder CF, Dodia C, Han J, Mesaros C, Shuvaev VV, Blair IA, Fisher AB, and Muzykantov VR (2012) Antioxidant protection by PECAM-targeted delivery of a novel NADPH-oxidase inhibitor to the endothelium *in vivo* and *in vivo*. J. Controlled Release 163 (2), 161–9.

(10). Howard MD, Greineder CF, Hood ED, and Muzykantov VR (2014) Endothelial targeting of liposomes encapsulating SOD/catalase mimetic EUK-134 alleviates acute pulmonary inflammation. J. Controlled Release 177, 34–41.

(11). Khoshnejad M, Shuvaev VV, Pulsipher KW, Dai C, Hood ED, Arguiri E, Christofidou-Solomidou M, Dmochowski IJ, Greineder CF, and Muzykantov VR (2016) Vascular Accessibility of Endothelial Targeted Ferritin Nanoparticles. Bio-conjugate Chem 27 (3), 628–37.

(12). Li R, Kowalski PS, Morselt HWM, Schepel I, Jongman RM, Aslan A, Ruiters MHJ, Zijlstra JG, Molema G, van Meurs M, et al. (2018) Endothelium-targeted delivery of dexamethasone by anti-VCAM-1 SAINT-O-Somes in mouse endotoxemia. PLoS One 13 (5), e0196976. [PubMed: 29763440]

(13). Torchilin VP (2005) Recent advances with liposomes as pharmaceutical carriers. Nat. Rev. Drug Discovery 4 (2), 145–60. [PubMed: 15688077]

(14). Paszko E, and Senge MO (2012) Immunoliposomes. Curr. Med. Chem 19 (31), 5239–5277. [PubMed: 22934774]

(15). Venditto VJ, and Szoka FC (2013) Cancer nanomedicines: So many papers and so few drugs! Adv. Drug Delivery Rev 65 (1), 80–88.

(16). Agarwal P, and Bertozzi CR (2015) Site-specific antibody-drug conjugates: the nexus of bioorthogonal chemistry, protein engineering, and drug development. Bioconjugate Chem 26 (2), 176–92.

(17). Blenke EO, Klaasse G, Merten H, Pluckthun A, and Mastrobattista E (2015) Liposome functionalization with copper-free ″click chemistry″. J. Controlled Release 202, 14–20.

(18). van der Geest T, Laverman P, Gerrits D, Franssen GM, Metselaar JM, Storm G, and Boerman OC (2015) Comparison of three remote radiolabelling methods for long-circulating liposomes. J. Controlled Release 220, 239–244.

(19). Molina Nunez M, de Alarcon R, Roca S, Alvarez G, Ros MS, Jimeno C, Bucalo L, Villegas I, and Garcia MA (2015) Citrate versus acetate-based dialysate in on-line haemodiafiltration. A prospective cross-over study. Blood Purif 39 (1–3), 181–7. [PubMed: 25791278]

(20). Niu G, Cogburn B, and Hughes J (2010) Preparation and characterization of doxorubicin liposomes. Methods Mol. Biol 624, 211–9. [PubMed: 20217598]

(21). Brenner JS, Kiseleva RY, Glassman PM, Parhiz H, Greineder CF, Hood ED, Shuvaev VV, and Muzykantov VR (2018) The new frontiers of the targeted interventions in the pulmonary vasculature: precision and safety (2017 Grover Conference Series). Pulm. Circ 8 (1), 204589321775232.

(22). Hood E, Simone E, Wattamwar P, Dziubla T, and Muzykantov V (2011) Nanocarriers for vascular delivery of antioxidants. Nanomedicine (London, U. K.) 6 (7), 1257–72.

(23). Howard MD, Hood ED, Zern B, Shuvaev VV, Grosser T, and Muzykantov VR (2014) Nanocarriers for vascular delivery of anti-inflammatory agents. Annu. Rev. Pharmacol. Toxicol 54, 205–26. [PubMed: 24392694]

(24). Muzykantov VR (2001) Delivery of antioxidant enzyme proteins to the lung. Antioxid. Redox Signaling 3 (1), 39–62.

(25). Simone E, Ding BS, and Muzykantov V (2009) Targeted delivery of therapeutics to endothelium. Cell Tissue Res 335 (1), 283–300. [PubMed: 18815813]

(26). Shuvaev VV, Muro S, Arguiri E, Khoshnejad M, Tliba S, Christofidou-Solomidou M, and Muzykantov VR (2016) Size and targeting to PECAM vs ICAM control endothelial delivery, internalization and protective effect of multimolecular SOD conjugates. J. Controlled Release 234, 115–23.

(27). Zern BJ, Chacko AM, Liu J, Greineder CF, Blankemeyer ER, Radhakrishnan R, and Muzykantov V (2013) Reduction of nanoparticle avidity enhances the selectivity of vascular targeting and PET detection of pulmonary inflammation. ACS Nano 7 (3), 2461–9. [PubMed: 23383962]

(28). Stephanopoulos N, and Francis MB (2011) Choosing an effective protein bioconjugation strategy. Nat. Chem. Biol 7 (12), 876–84. [PubMed: 22086289]

(29). Greineder CF, Hood ED, Yao A, Khoshnejad M, Brenner JS, Johnston IH, Poncz M, Gottstein C, and Muzykantov VR (2016) Molecular engineering of high affinity single-chain antibody fragment for endothelial targeting of proteins and nanocarriers in rodents and humans. J. Controlled Release 226, 229–237.

(30). Greineder CF, Villa CH, Walsh LR, Kiseleva RY, Hood ED, Khoshnejad M, Warden-Rothman R, Tsourkas A, and Muzykantov VR (2018) Site-Specific Modification of Single-Chain Antibody Fragments for Bioconjugation and Vascular Immunotargeting. Bioconjugate Chem 29 (1), 56–66.

(31). Yumura K, Ui M, Doi H, Hamakubo T, Kodama T, Tsumoto K, and Sugiyama A (2013) Mutations for decreasing the immunogenicity and maintaining the function of core streptavidin. Protein Science: A Publication of the Protein Society 22 (2), 213–221.

(32). Parker CL, Yang Q, Yang B, McCallen JD, Park SI, and Lai SK (2017) Multivalent interactions between streptavidin-based pretargeting fusion proteins and cell receptors impede efficient internalization of biotinylated nanoparticles. Acta Biomater 63, 181–189. [PubMed: 28870833]

(33). Shuvaev VV, Dziubla T, Wiewrodt R, and Muzykantov VR (2004) Streptavidin-biotin crosslinking of therapeutic enzymes with carrier antibodies: nanoconjugates for protection against endothelial oxidative stress. Bioconjugation Protocols 283, 3–19.

(34). Lallana E, Sousa-Herves A, Fernandez-Trillo F, Riguera R, and Fernandez-Megia E (2012) Click Chemistry for Drug Delivery Nanosystems. Pharm. Res 29 (1), 1–34. [PubMed: 21913032]

(35). Lutz JF, and Zarafshani Z (2008) Efficient construction of therapeutics, bioconjugates, biomaterials and bioactive surfaces using azide-alkyne ″click″ chemistry. Adv. Drug Delivery Rev 60 (9), 958–970.

(36). Marques-Gallego P, and de Kroon AIPM (2014) Ligation Strategies for Targeting Liposomal Nanocarriers. BioMed Res. Int 2014, 129458. [PubMed: 25126543]

(37). Said Hassane F, Frisch B, and Schuber F (2006) Targeted liposomes: convenient coupling of ligands to preformed vesicles using ″click chemistry″. Bioconjugate Chem 17 (3), 849–54.

(38). Zhang H, Ma Y, and Sun XL (2009) Chemically-selective surface glyco-functionalization of liposomes through Staudinger ligation. Chem. Commun. (Cambridge, U. K.) 21, 3032–4.

(39). Gaetke LM, and Chow CK (2003) Copper toxicity, oxidative stress, and antioxidant nutrients. Toxicology 189 (1–2), 147–63. [PubMed: 12821289]

(40). Jewett JC, and Bertozzi CR (2010) Cu-free click cycloaddition reactions in chemical biology. Chem. Soc. Rev 39 (4), 1272–1279. [PubMed: 20349533]

(41). Bak M, Jolck RI, Eliasen R, and Andresen TL (2016) Affinity Induced Surface Functionalization of Liposomes Using Cu-Free Click Chemistry. Bioconjugate Chem 27 (7), 1673–1680.

(42). van Lith SAM, van Duijnhoven SMJ, Navis AC, Leenders WPJ, Dolk E, Wennink JWH, van Nostrum CF, and van Hest JCM (2017) Legomedicine—A Versatile Chemo-Enzymatic Approach for the Preparation of Targeted Dual-Labeled Llama Antibody–Nanoparticle Conjugates. Bioconjugate Chem 28 (2), 539–548.

(43). Silindir M, Erdoğan S,Özer AY, Doğan AL, Tuncel M, Ugur Ö, and Torchilin VP (2013) Nanosized multifunctional liposomes for tumor diagnosis and molecular imaging by SPECT/CT. J. Liposome Res 23 (1), 20–27. [PubMed: 23078019]

(44). Chi L, Na M-H, Jung H-K, Vadevoo SMP, Kim C-W, Padmanaban G, Park T-I, Park J-Y, Hwang I, Park KU, et al. (2015) Enhanced delivery of liposomes to lung tumor through targeting interleukin-4 receptor on both tumor cells and tumor endothelial cells. J. Controlled Release 209, 327–336.

(45). Greineder CF, Johnston IH, Villa CH, Gollomp K, Esmon CT, Cines DB, Poncz M, and Muzykantov VR (2017) ICAM-1-targeted thrombomodulin mitigates tissue factor-driven inflammatory thrombosis in a human endothelialized microfluidic model. Blood Adv 1 (18), 1452–1465. [PubMed: 29296786]

(46). Kiseleva R, Greineder CF, Villa CH, Hood ED, Shuvaev VV, Sun J, Chacko AM, Abraham V, DeLisser HM, and Muzykantov VR (2017) Mechanism of Collaborative Enhancement of Binding of Paired Antibodies to Distinct Epitopes of Platelet Endothelial Cell Adhesion Molecule-1. PLoS One 12 (1), e0169537. [PubMed: 28085903]

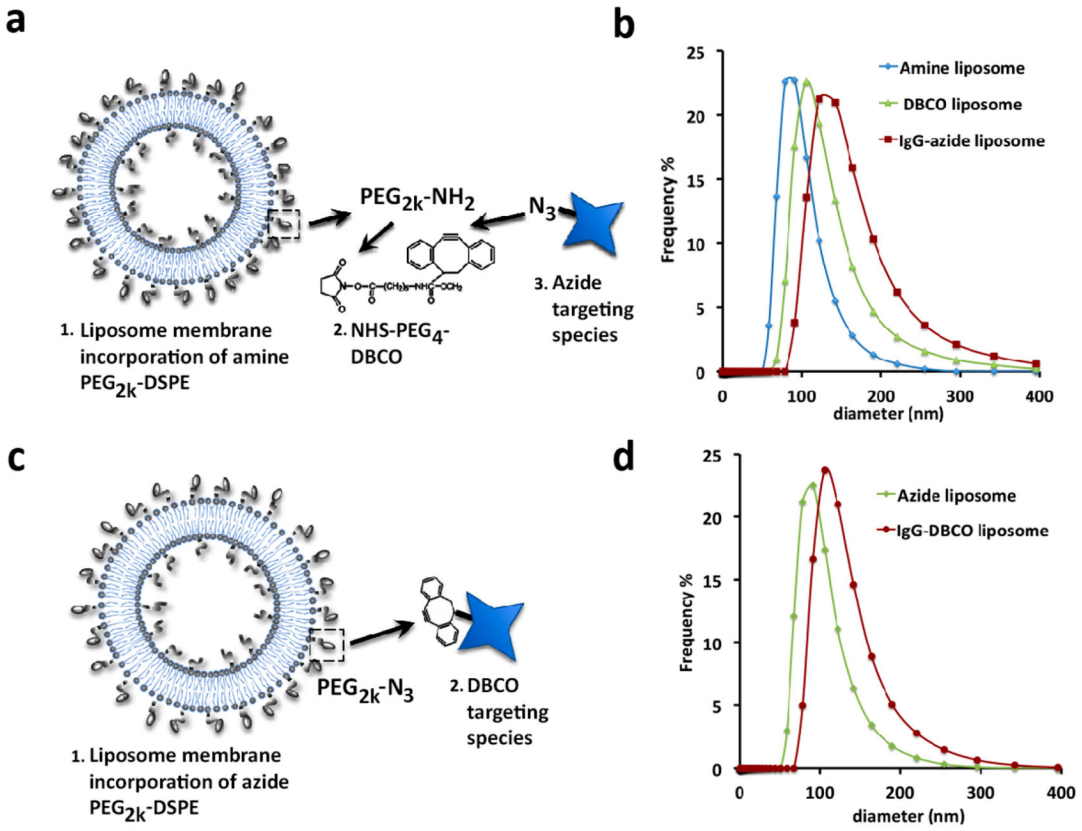

Figure 1.

Dual modally functionalized click liposomes. (a) DBCO functionalized liposome conjugation scheme. (b) Particle size distribution of amine/DBCO and IgG azide labeled liposomes at each stage of targeting functionalization. (c) Azide functionalized liposome conjugation scheme. (d) Particle size distribution of azide liposomes before and after IgG-DBCO conjugation.

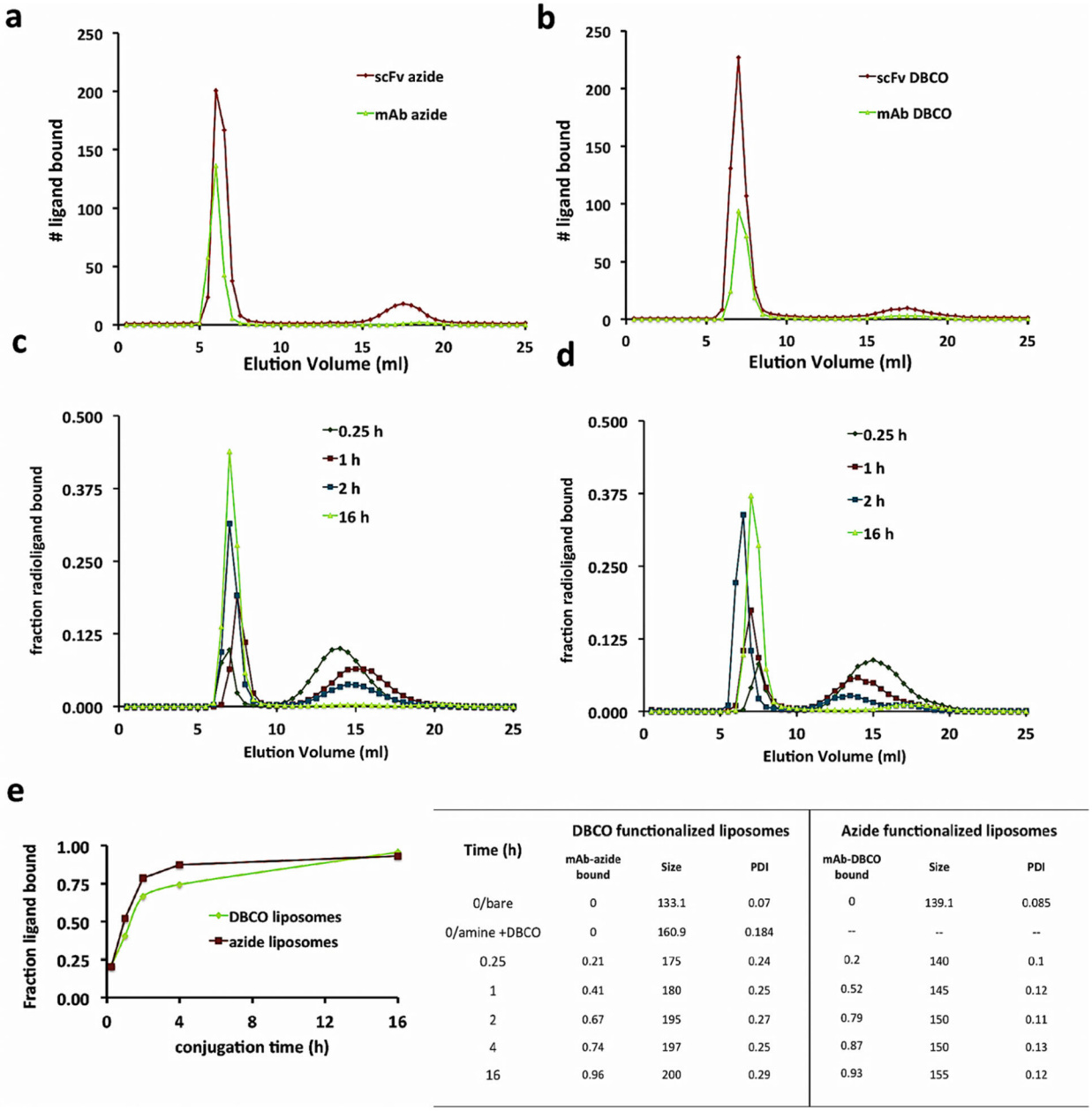

Time (h)	DBCO functionalized liposomes			Azide functionalized liposomes		
	mAb-azide bound	Size	PDI	mAb-DBCO bound	Size	PDI
0/bare	0	133.1	0.07	0	139.1	0.085
0/amine +DBCO	0	160.9	0.184	--	--	--
0.25	0.21	175	0.24	0.2	140	0.1
1	0.41	180	0.25	0.52	145	0.12
2	0.67	195	0.27	0.79	150	0.11
4	0.74	197	0.25	0.87	150	0.13
16	0.96	200	0.29	0.93	155	0.12

Figure 2.

Dual modal click-functionalization of liposomes enables conjugation of varied endothelial adhesion molecule targeting species. (a,b) Gel exclusion chromatography elution data of (a) DBCO liposomes incubated with ^{125}I-azide functionalized mAb (green line) or scFv (red line) and (b) azide liposomes, as labeled in (a). The early elution peak (5–7 mL) in both graphs signals the radioactive ligand bound to the liposome, and the later peaks (max peak 14 mL for mAb, 17.5 mL for scFv) signals the unbound ligand elution signal. The y-axis # ligand bound calculated from a known addition of ligands, with scFv azide/DBCO species added 2.0× greater than mAb DBCO/azide. Area under the curve analyses of elution graphs calculate 85–95% conjugation efficiency. (c,d) Kinetics data of azide/DBCO modified IgG conjugation reaction to DBCO/azide functionalized liposomes. ^{125}I labeled IgG-azide/

DBCO traced as in a,b. (e) Comparison of bound ligand over time by click species orientation. (f) Extent of bound ligands, particle size, and PDI of kinetics data samples shown in c,d.

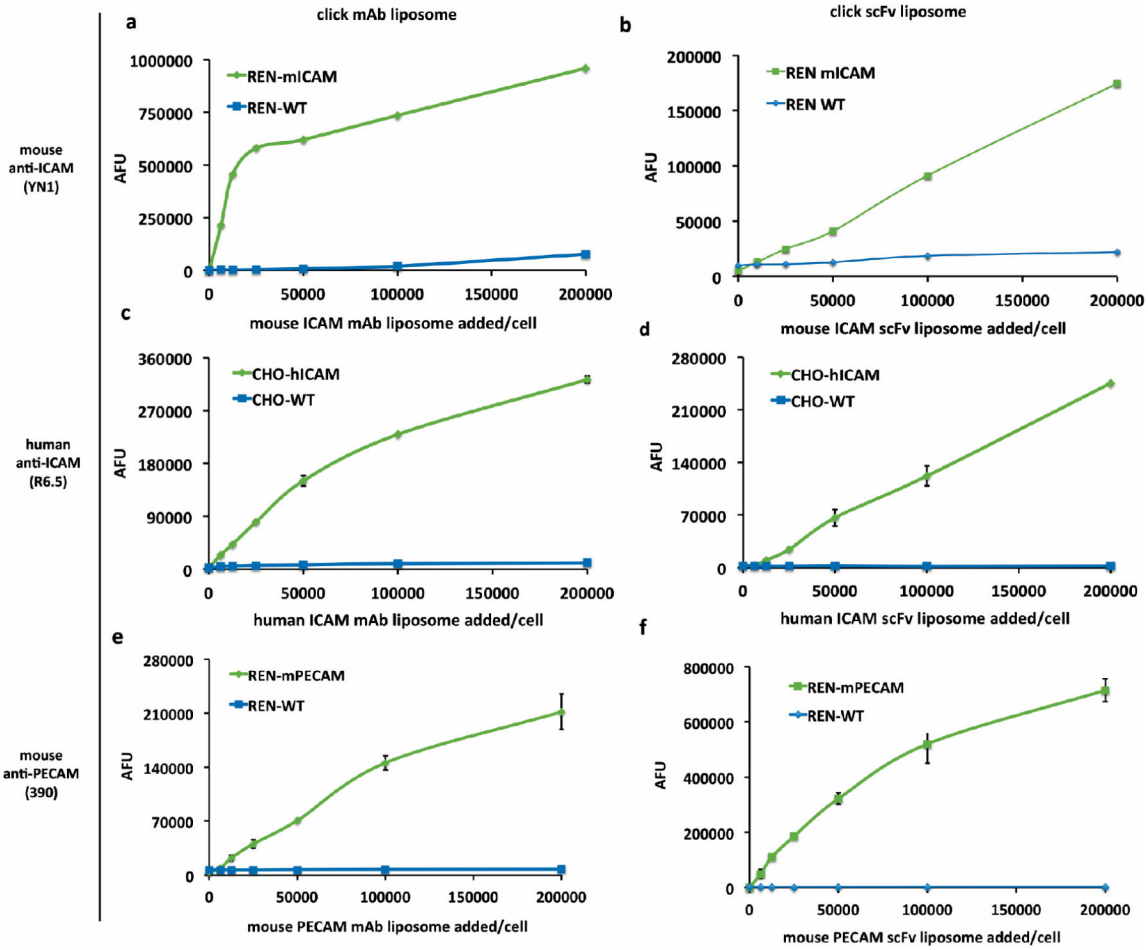

Figure 3.

In vivo binding of CAM targeted click liposomes shows specificity to target cells vs wild type cells. Flow cytometry data graphed as mean fluorescence values of scFv and mAb click conjugated fluorescent liposomes targeted to designated CAMs at varying concentrations. (a,b) YN1 mAb (a) and scFv (b) liposomes binding to REN mouse ICAM cells versus REN WT. (c,d) R6.5 mAb (c) and scFv (d) liposomes show specific binding to CHO human ICAM cells versus CHO WT. (e,f) 390 mAb (e) and scFv (f) liposomes binding to REN mouse PECAM cells versus REN WT. Error bars represent standard deviation, $n = 2$.

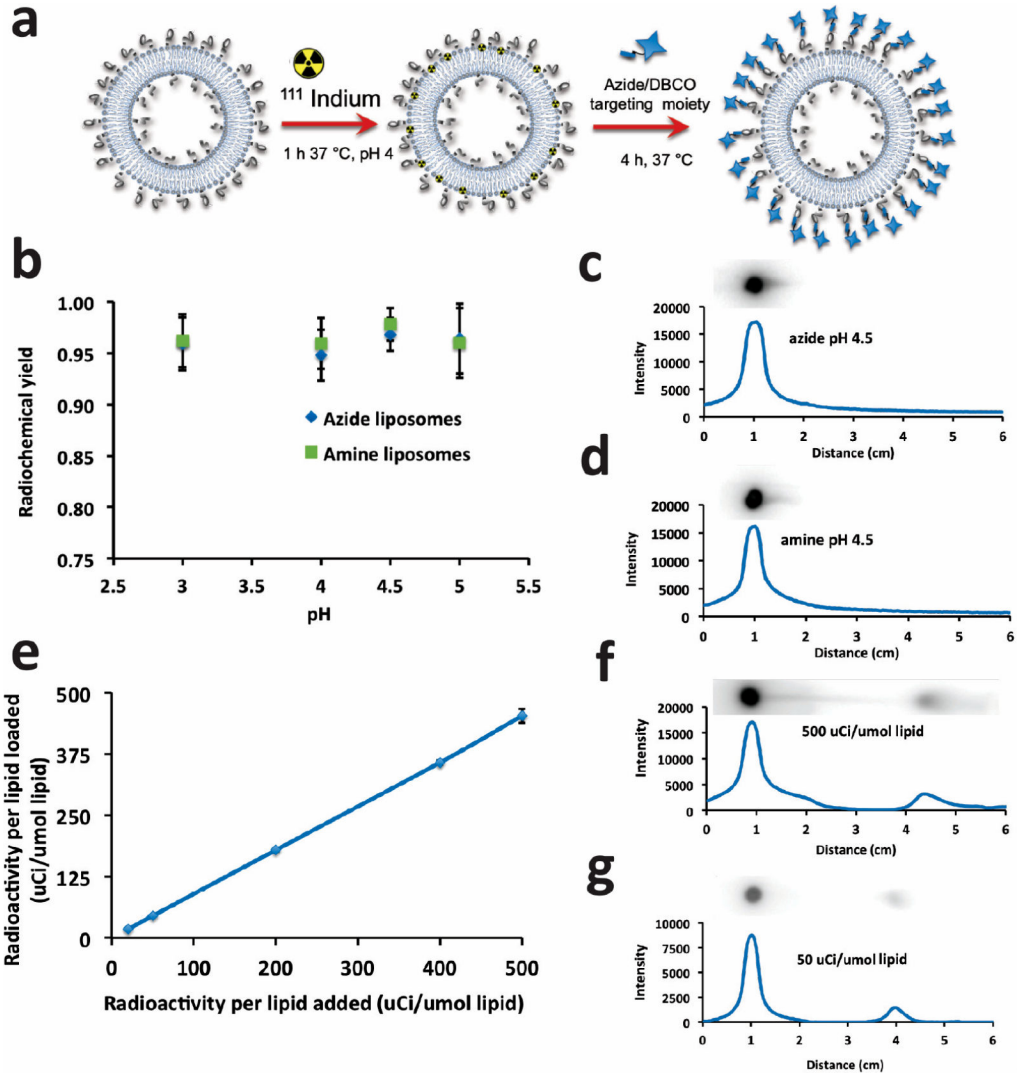

Figure 4.

^{111}In labeling of clickable liposomes. (a) Schematic of labeling procedure. (b) Gamma quantification (origin vs total) of thin layer chromatography of unpurified, quenched amine and azide liposome reaction mixtures with range of pH 3–5. (c,d) Autoradiography of phosphor gel scan of representative TLC thin layer at pH 4.5 for each liposome type. Graphs represent gray scale intensity vs migration of reactive species from origin in EDTA mobile phase. (e) Radiochemical yield vs μCi activity loaded into azide liposomes demonstrates linear radiochemical yield and purity (~90% without purification) with no indication of reaching saturation. (f,g) Autoradiography and TLC quantification as in c and d of data from (e) of high (f) and low (g) addition. Phosphor TLC imaging corresponds with gamma counting.

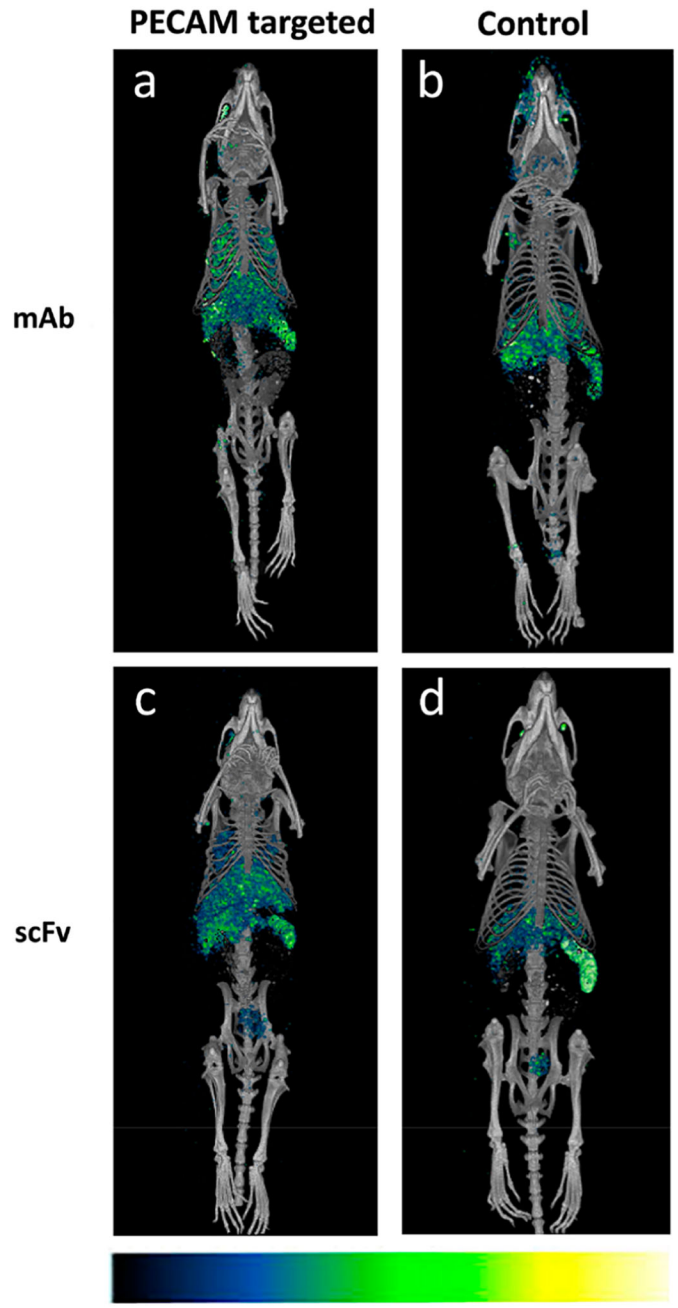

Figure 5.

MicroSPECT-CT images of ^{111}In anti PECAM radioimmunoliposome show pulmonary localization PECAM vs control. Images acquired 30 min post injection of PECAM mAb (a), IgG (b), PECAM scFv (c), or nonspecific scFv (d) click radioimmunoliposome. Pseudocolor scale inset at bottom shows signal intensity increasing from left to right.

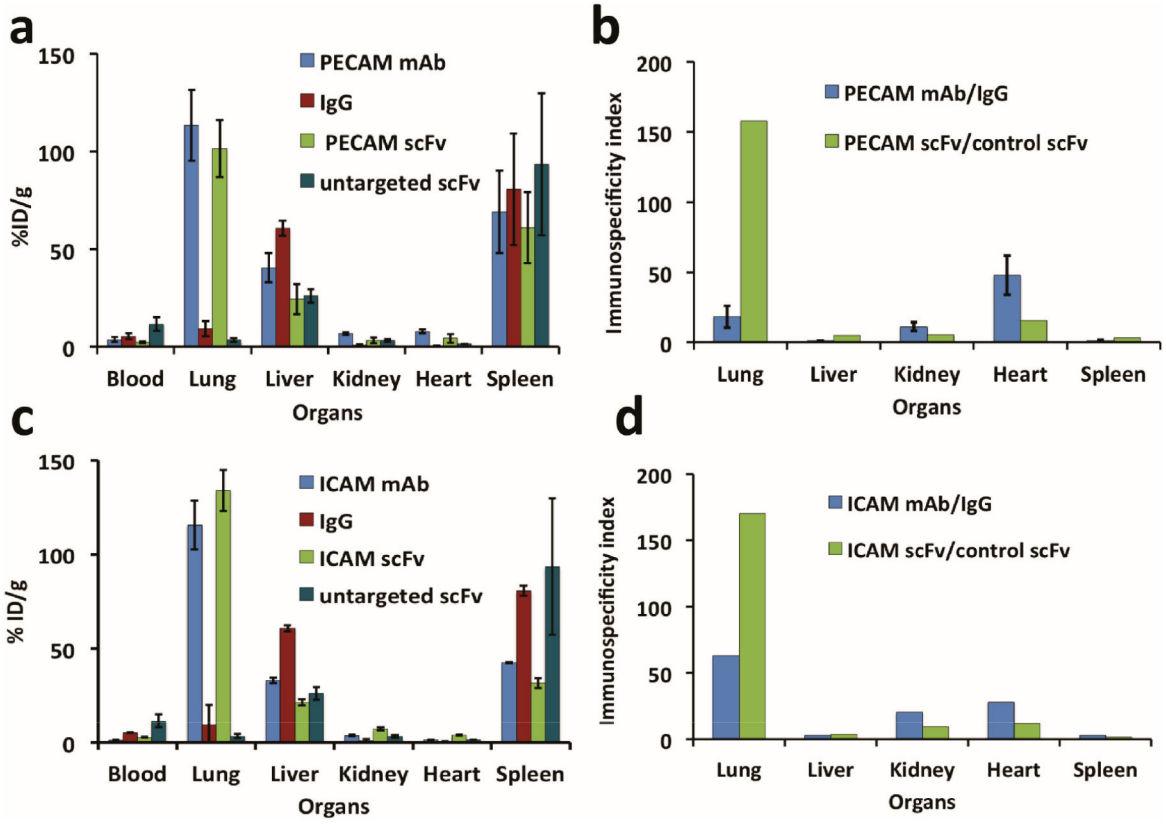

Figure 6.

Highly selective *in vivo* endothelial targeting of ^{111}In labeled anti CAM mAb and scFv click radioimmunoliposome. Biodistribution of ^{111}In labeled anti PECAM liposomes injected in Naïve mice 30 min after administration by injected dose per gram of tissue. (a) Mouse PECAM (clone 390) click radioimmunoliposome of mAb (blue) and scFv (green) accumulation by organ versus untargeted immune controls IgG (red) and untargeted scFv (teal). (b) Immunospecificity index, the ratio of signal localized in organs normalized to blood signal of targeted to control click radioimmunoliposome, of data in (a). (c) Biodistribution of ICAM (clone YN1) targeting of mAb and scFv as in (a) and (d) immunospecificity as in (b). Error bars represent standard deviation, $n \geq 3$–4.